

# Phase shifting electronic speckle pattern interferometry (ESPI) with unresolved speckle

Volkmar Eichhorn, Heinz Helmers

Carl von Ossietzky Universität Oldenburg, Institut für Physik  
D-2611 Oldenburg

<mailto:heinz.helmers@uni-oldenburg.de>

We present experimental data that enable a quantitative determination of the figure of merit of ESPI correlation fringes and phase maps for a set-up using unresolved speckle. Furthermore we discuss a variant of the spatial phase shifting technique applied to this case.

## 1 Introduction

Electronic speckle pattern interferometry (ESPI) is usually realized with resolved speckle. In that case the mean speckle size approximately equals the pixel size of the CCD- or CMOS-sensor. This is achieved by using a small aperture of the objective which simultaneously reduces the intensity of the object light. If the laser power is limited and large objects are to be illuminated, the aperture must be opened in order to ensure a sufficient exposure of the sensor. Thereby the speckle become smaller and every pixel integrates over  $n$  speckle with random intensity and phase. However, even in this case speckle interferometry is possible, as was shown theoretically by Lehmann [1]. We present experimental data that enable a quantitative comparison of the figure of merit of correlation fringes and phase maps as a function of  $n$ . Furthermore we present a variant of the spatial phase shifting technique applied to ESPI with unresolved speckle.

## 2 Figure of merit for correlation fringes

In the simplest case the result of an ESPI deformation measurement is a system of correlation fringes ("subtraction image"). The quality of such fringes can be described by their visibility  $V$ . Because correlation fringes are disturbed by speckle noise,  $V$  cannot be measured directly. However, if parallel and equidistant fringes are analyzed,  $V$  can be calculated from the visibility  $V_A$  of the corresponding autocorrelation function (ACF):  $V = \sqrt{2 V_A}$ . The advantage of this procedure is that  $V_A$  can be determined straightforward because the ACF is free of speckle noise due to the integration process. Fig. 1 (left) shows an example.

## 3 Figure of merit for sawtooth phase maps

By the application of spatial or temporal phase shifting techniques (SPS or TPS) sawtooth fringes are generated as the result of ESPI deformation

measurements. Again, if parallel and equidistant fringes are analyzed, an ideal sawtooth fringe system can be found by the downhill simplex algorithm which represents a best fit to the measured fringe system [2]. The figure of merit of the sawtooth phase map is then defined as the rms-difference between the measured and the ideal phase map. This quantity is called the phase noise  $N$ . Fig. 1 (right) shows an example.

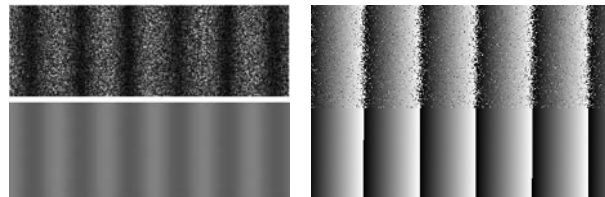


Fig. 1 Left: Correlation fringes (top) and their ACF (bottom). Right: Sawtooth fringes (top) and corresponding fit (bottom).

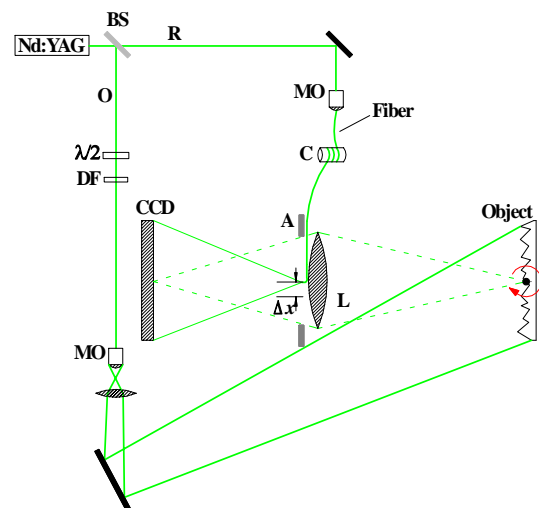


Fig. 2 : Experimental set-up of the ESPI system

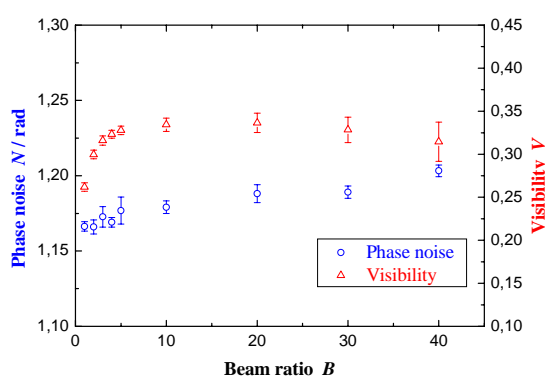
## 4 Experimental set-up

Fig. 2 shows the set-up used for the investigations. The reference wave R is guided by a fiber. For the

application of temporal phase shifting (TPS) the phase of R can be changed by stretching the piezo-electric cylinder C. The beam ratio  $B = I_{Ref} / \langle I_{Obj} \rangle$  is adjusted with the variable beam splitter BS and the density filter DF. The speckle size is controlled by the diameter of the stop A in front of the objective lens L. The object can be rotated precisely by a piezo-electric actuator in order to generate parallel and equidistant deformation fringes.

## 5 Results

Fig. 3 shows that for unresolved speckle (here:  $n \approx 14.2$ ) only a weak dependence exists between the beam ratio  $B$  and the visibility  $V$  or the phase noise  $N$ . Similar results were achieved in previous investigations for resolved speckle [3].



**Fig. 3 :** Visibility  $V$  and phase noise  $N$  as function of the beam ratio  $B$ .

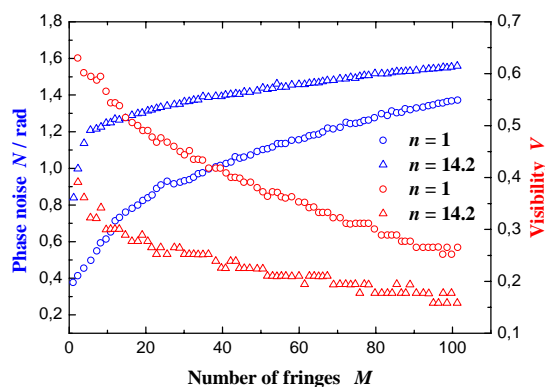


**Fig. 4 :** Visibility  $V$  and phase noise  $N$  as a function of the number of fringes  $M$  for different numbers of speckle per pixel,  $n$ .

Fig. 4 shows  $V$  and  $N$  (for  $B \approx 10$ ) as a function of the number of vertical fringes,  $M$ , for different  $n$ . Finally, Fig. 5 shows  $V$  and  $N$  as a function of  $n$  (for  $B \approx 10$  and  $M \approx 7.2$ ). The results prove the theoretical prediction that also in the case of unresolved speckle ESPI can deliver phase maps of sufficient quality in order to determine object deformations. On the other hand, the course of the curves in Fig 4 and 5 cannot be described

satisfactory with available models [1,4]. Therefore further work has to be done in order to understand the measured behaviour in more detail.

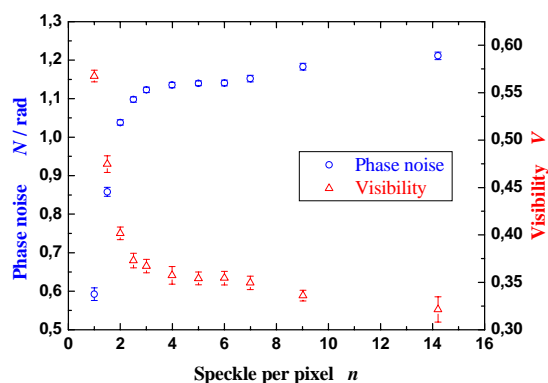


**Fig. 5 :** Visibility  $V$  and phase noise  $N$  as function of the number of speckle per pixel  $n$ .

## 6 SPS with unresolved speckle

SPS as described in [2] requires the phase of the object wave to be nearly constant over 3 neighbouring pixel of the sensor. For unresolved speckle this prerequisite is violated. However, some advantages of SPS can be used in this case too. For this purpose the fiber guiding the reference wave R is shifted by  $\Delta x$  (see Fig. 3) after recording the speckle interferogram  $I_1$  of the first object state. This leads to a corresponding change of the phase of R at the sensor (here:  $\approx 120^\circ/\text{column}$ ). After that the speckle interferograms  $I_i$  of the following object states  $O_i$  are recorded. From each difference  $I_i - I_1$  three phase shifted correlation fringe systems can be calculated and from these after suitable filtering the sawtooth phase maps. First results are presented in Fig. 6. They still show some deviations in the reconstructed phase maps. A considerable improvement is expected by proper alignment of the phase front of R which wasn't done yet now.



**Fig. 6 :** Sawtooth fringes for  $n = 1, 3, 7, 14.2$  (from left to right).

## References

- [1] M. Lehmann: Opt. Commun. 128 (1996) 325-340
- [2] J. Burke, H. Helmers et al.: Opt. Commun. 152.1-3 (1998) 144-152
- [3] J. Burke, H. Helmers: Appl. Opt. 39.25 (2000) 4598-4606
- [4] M. Owner-Petersen: J. Opt. Soc. Am. A 8.7 (1991) 1082-1089